A study on an optimal movement model

2003 J. Phys. A: Math. Gen. 36 7469

(http://iopscience.iop.org/0305-4470/36/27/301)

INSTITUTE OF PHYSICS PUBLISHING JOURNAL OF PHYSICS A: MATHEMATICAL AND GENERAL

J. Phys. A: Math. Gen. **36** (2003) 7469–7484 PII: S0305-4470(03)60258-1

A study on an optimal movement model

Jianfeng Feng[1], **Kewei Zhang**[2] **and Yousong Luo**[3]

[1] COGS, Sussex University, Brighton BN1 9QH, UK
[2] SMS, Sussex University, Brighton BN1 9QH, UK
[3] Department of Mathematics and Statistics, RMIT University, GOP Box 2476V, Melbourne, Vic 3001, Australia

Received 26 February 2003, in final form 20 May 2003
Published 25 June 2003
Online at stacks.iop.org/JPhysA/36/7469

Abstract

We present an analytical and rigorous study on a TOPS (task optimization in the presence of signal-dependent noise) model with a hold-on or an end-point control. Optimal control signals are rigorously obtained, which enables us to investigate various issues about the model including its trajectories, velocities, control signals, variances and the dependence of these quantities on various model parameters. With the hold-on control, we find that the optimal control can be implemented with an almost 'nil' hold-on period. The optimal control signal is a linear combination of two sub-control signals. One of the sub-control signals is positive and the other is negative. With the end-point control, the end-point variance is dramatically reduced, in comparison with the hold-on control. However, the velocity is not symmetric (bell shape). Finally, we point out that the velocity with a hold-on control takes the bell shape only within a limited parameter region.

PACS numbers: 05.40.Jc, 02.50.−r, 05.90.+m, 84.35.+i, 87.19.La

(Some figures in this article are in colour only in the electronic version)

1. Introduction

The earliest TOPS (task optimization in the presence of signal-dependent noise) model was first proposed in [9] and since then it has been intensively investigated in the literature, both in experiments (see, for example, some are reviews [7, 10–13, 15, 18, 22, 25, 26, 29]) and in theory [6, 21, 24, 27]. Various interesting versions of the model have also been put forward (see aforementioned reviews). Basically, in the TOPS model, we intend to minimize the variance of the trajectory in a specified time window. For example, in the first TOPS model [9], the variance of post-movement within time window $[T, T + R]$ is minimized, where T is the time the eye or arm has arrived at its goal and $R > 0$ is the length of optimization time window. Despite the wide interests in the model, no analytical solution of various TOPS

models has been reported, and so it remains a difficult issue to fully understand the behaviour of models [21]. In the current paper we provide a rigorous approach and the analytical solution of the TOPS model is found. We confine ourselves to the simplest model studied in [9], but our approach is general enough to tackle other related models as well.

It is one of the puzzling issues in the neuroscience that why neuron fires randomly (an issue related to rate coding and time coding [8, 16, 23]). With deterministic inputs and outputs, the required resourses for carrying out a computation in the nervous system can be significantly reduced. It is claimed that the TOPS model might reveal one functional role of random activity widely observed in the nervous system. By modelling saccadic movements and arm movements, it is found that the velocity profile obtained from TOPS models fits well with experimental data, i.e. it takes the bell shape.

Although the TOPS model provides us with an excellent explanation on stochastic neuron firings, at the same time, it introduces many other issues to explain. As usual, a successful theory only serves to raise a whole set of new questions. For example, why does the velocity profile exhibit the bell shape? Which key mechanism determines the output? How does the model behaviour depend on various model parameters?

By solving the model theoretically, we answer all aforementioned questions. We find that the optimal control signal is a linear combination of two control signals: one is positive and the other is negative. The result about the combination of two signals tells us how to realize input signals via actual neuron outputs. Remembering that in the nervous system, a neuron is either excitatory or inhibitory.

How does the control signal depend on the hold-on period? From numerical simulations, it seems a certain amount of hold-on period is required to correctly perform the task, or to produce the bell shape velocity. We find that the hold-on period could be as short as possible: it could even approach to zero. We then check the variability of the velocity and trajectory of the model. Furthermore, we point out that the hold-on constraint is equivalent to an instantaneous constraint: to require that the velocity vanishes when the trajectory arrives at the desired position. It is found that the bell shape velocity is partly from the assumption of zero velocity at the end of movement, or the hold-on constraint.

To gain a further understanding of the hold-on control, we then consider a control problem with an end-point control of variance. It is found that the variance of the trajectory with the end-point control is considerably reduced, in comparison with the hold-on control. However, the property of symmetric velocity is no longer true. This also leads us to further ask another question: whether the symmetric velocity is a natural consequence of the TOPS model or not? Unfortunately, we find that the velocity profile depends on model parameters: with a short period of movement (T is small), the velocity is symmetric; but with a long period of movement, the velocity is no longer symmetric.

The paper is organized as follows. In section 2, the model is introduced. In section 3, we consider the hold-on control problem. An analytical solution of the problem is obtained and various properties of the solution are discussed. The equivalence between the hold-on constraint and an instantaneous constraint on trajectory and velocity is established. In section 4, we turn our attention to the end-point control problem and a comparison between the hold-on and the end-point control is carried out.

This is the third in our series of papers on biological control problems. In [6], we have found the analytical solution without hold-on constraints. In [5], we have investigated the input signals used in the TOPS model. In the near future, we are going to carry out a study on arm movement models and more physiologically realistic models. Our aim is to establish an integrated system: to build models from sensory inputs to neuronal outputs and from neuronal outputs to motor outputs.

2. Model

We consider a simple model of saccadic movements. Let $x_1(t)$ be the position of the eye (in degrees) and $x_2(t)$ be its velocity (degree/s), we then have

$$\begin{cases} \dot{x}_1 = x_2 \\ \dot{x}_2 = -\frac{1}{\tau_1\tau_2}x_1 - \frac{\tau_1+\tau_2}{\tau_1\tau_2}x_2 + \frac{1}{\tau_1\tau_2}\bar{u} \end{cases} \tag{2.1}$$

where τ_1, τ_2 are parameters and $\bar{u}$ is the input signal as defined below. However, we are more interested in general principles rather than numerically fitting of experimental data. From now on, we assume that all parameters are in arbitrary units, although a fitting would be straightforward. In matrix terms we have

$$\mathrm{d}\vec{X}_t = A\vec{X}_t\,\mathrm{d}t + \mathrm{d}\vec{U}_t \tag{2.2}$$

where

$$A = \begin{pmatrix} 0 & 1 \\ -\frac{1}{\tau_1\tau_2} & -\frac{\tau_1+\tau_2}{\tau_1\tau_2} \end{pmatrix} \tag{2.3}$$

and

$$\mathrm{d}\vec{U}_t = \begin{pmatrix} 0 \\ \frac{u(t)\,\mathrm{d}t + u(t)^\alpha\,\mathrm{d}B_t}{\tau_1\tau_2} \end{pmatrix}$$

with B_t being Brownian motions, $u(t)$ the control signal and $\alpha > 0$. The importance of α has been discussed in [5] and we refer the reader to it for details. Basically, under the rate coding assumption, $\alpha = 1/2$ corresponds to the Poisson inputs [20, 28]. With time coding assumption, $\alpha = 1$ is the Poisson input.

The meaning of equation (2.1) is quite clear, corresponding to the well-known Kramers' equation which is defined by

$$\begin{cases} \mathrm{d}X_t = V_t\,\mathrm{d}t \\ \mathrm{d}V_t = -\partial H(X_t, t)/\partial X_t\,\mathrm{d}t - \eta_1 V_t\,\mathrm{d}t + \eta_2(t)\,\mathrm{d}B_t \end{cases}$$

where η_1 (viscosity) and $\eta_2(t)$ are deterministic functions, X_t is the position, V_t is the velocity and H is the potential. Usually, in the literature $H(x, t)$ is a function dependent only on x. However, in our set-up, H depends on both t and x and is thus nonhomogeneous in time.

Solving equation (2.1) we obtain that

$$\begin{aligned} \vec{X}_t &= \int_0^t \exp(A(t-s))\,\mathrm{d}\vec{U}_t \\ &= \int_0^t \left[\begin{pmatrix} \frac{b_{12}(t-s)}{\tau_1\tau_2}u(s)\,\mathrm{d}s \\ \frac{b_{22}(t-s)}{\tau_1\tau_2}u(s)\,\mathrm{d}s \end{pmatrix} + \begin{pmatrix} \frac{b_{12}(t-s)}{\tau_1\tau_2}u^\alpha(s)\,\mathrm{d}B_s \\ \frac{b_{22}(t-s)}{\tau_1\tau_2}u^\alpha(s)\,\mathrm{d}B_s \end{pmatrix} \right] \end{aligned} \tag{2.4}$$

where $b_{ik}(t-s) = (\exp(A(t-s)))_{ik}$, $i, k = 1, 2$.

Note that

$$\left\langle \int_T^{T+R} \left[\int_0^t b_{12}(t-s)u(s)^\alpha\,\mathrm{d}B_s \right]^2 \mathrm{d}t \right\rangle = \int_T^{T+R} \left[\int_0^t b_{12}^2(t-s)u(s)^{2\alpha}\,\mathrm{d}s \right] \mathrm{d}t \tag{2.5}$$

where B_s is the standard Brownian motion. The original control problem studied in [9] is reduced to the following optimization problem.

Hold-on control. Find $u(s) \in \mathcal{L}^{2\alpha}[0, T+R]$ which minimizes

$$\int_T^{T+R} \left[\int_0^t b_{12}^2(t-s)u(s)^{2\alpha}\,\mathrm{d}s \right] \mathrm{d}t \tag{2.6}$$

subject to the constraint

$$\int_0^t b_{12}(t-s)u(s)\,\mathrm{d}s = \tau_1\tau_2 D \qquad \text{for} \quad t \in [T, T+R]. \tag{2.7}$$

In all numerical simulations below, we fix $\tau_1 = 10$ and $\tau_2 = 100$.

3. Hold-on control

It is easily seen that the eigenvalues for matrix A defined by equation (2.3) is

$$\lambda = \begin{cases} -1/\tau_1 \\ -1/\tau_2 \end{cases} \tag{3.1}$$

with eigenvectors $v_1 = (1, -1/\tau_1)'$ and $v_2 = (1, -1/\tau_2)'$ correspondingly. Let

$$\mathcal{B} = (v_1, v_2) = \begin{pmatrix} 1 & 1 \\ -\frac{1}{\tau_1} & -\frac{1}{\tau_2} \end{pmatrix} \tag{3.2}$$

we then have

$$\exp(A(t-s)) = \mathcal{B}\begin{pmatrix} \exp\left(-\frac{1}{\tau_1}(t-s)\right) & 0 \\ 0 & \exp\left(-\frac{1}{\tau_2}(t-s)\right) \end{pmatrix}\mathcal{B}^{-1} \tag{3.3}$$

and

$$\begin{cases} b_{12}(t-s) = \frac{\tau_1\tau_2}{\tau_2-\tau_1}\left[\exp\left(-\frac{1}{\tau_2}(t-s)\right) - \exp\left(-\frac{1}{\tau_1}(t-s)\right)\right] \\ b_{22}(t-s) = \frac{\tau_1\tau_2}{\tau_2-\tau_1}\left[\frac{1}{\tau_1}\exp\left(-\frac{1}{\tau_1}(t-s)\right) - \frac{1}{\tau_2}\exp\left(-\frac{1}{\tau_2}(t-s)\right)\right]. \end{cases} \tag{3.4}$$

The mean position and mean velocity are thus given by

$$\begin{cases} \langle x_1(t)\rangle = \frac{1}{\tau_2-\tau_1}\int_0^t\left[\exp\left(-\frac{1}{\tau_2}(t-s)\right) - \exp\left(-\frac{1}{\tau_1}(t-s)\right)\right]u(s)\,\mathrm{d}s \\ \langle x_2(t)\rangle = \frac{1}{\tau_2-\tau_1}\int_0^t\left[\frac{1}{\tau_1}\exp\left(-\frac{1}{\tau_1}(t-s)\right) - \frac{1}{\tau_2}\exp\left(-\frac{1}{\tau_2}(t-s)\right)\right]u(s)\,\mathrm{d}s \end{cases} \tag{3.5}$$

for $t \in [0, T+R]$. Note that the constraint

$$\int_0^t b_{12}(t-s)u(s)\,\mathrm{d}s = D\tau_1\tau_2$$

for $t \in [T, T+R]$ is equivalent to

$$\exp\left(-\frac{t}{\tau_2}\right)\int_0^t \exp\left(\frac{s}{\tau_2}\right)u(s)\,\mathrm{d}s - \exp\left(-\frac{t}{\tau_1}\right)\int_0^t \exp\left(\frac{s}{\tau_1}\right)u(s)\,\mathrm{d}s = (\tau_2-\tau_1)D \tag{3.6}$$

for $t \in [T, T+R]$. Since $R > 0$, by differentiating (3.6) with respect to t, we obtain

$$-\frac{1}{\tau_2}\exp\left(-\frac{t}{\tau_2}\right)\int_0^t \exp\left(\frac{s}{\tau_2}\right)u(s)\,\mathrm{d}s + \frac{1}{\tau_1}\exp\left(-\frac{t}{\tau_1}\right)\int_0^t \exp\left(\frac{s}{\tau_1}\right)u(s)\,\mathrm{d}s = 0 \tag{3.7}$$

for $t \in (T, T+R)$. Solving equations (3.6) and (3.7), we see that

$$\begin{cases} \int_0^t \exp\left(\frac{s}{\tau_2}\right)u(s)\,\mathrm{d}s = D\tau_2\exp\left(\frac{t}{\tau_2}\right) \\ \int_0^t \exp\left(\frac{s}{\tau_1}\right)u(s)\,\mathrm{d}s = D\tau_1\exp\left(\frac{t}{\tau_1}\right) \end{cases} \tag{3.8}$$

for $t \in [T, T+R]$, which implies that

$$u(t) = D \tag{3.9}$$

and in particular

$$\begin{cases} \int_0^T \exp\left(\frac{s}{\tau_2}\right) u(s)\,\mathrm{d}s = D\tau_2 \exp\left(\frac{T}{\tau_2}\right) \\ \int_0^T \exp\left(\frac{s}{\tau_1}\right) u(s)\,\mathrm{d}s = D\tau_1 \exp\left(\frac{T}{\tau_1}\right). \end{cases} \tag{3.10}$$

In fact, equation (3.9) can be directly derived from the model under the hold-on constraint.

It is easily seen that

$$\begin{aligned} I(u) &= \int_T^{T+R} \int_0^t b_{12}^2(t-s)|u(s)|^{2\alpha}\,\mathrm{d}s\,\mathrm{d}t \\ &= \int_0^T \left[\int_0^{T+R} b_{12}^2(t-s)\,\mathrm{d}t\right] u^{2\alpha}(s)\,\mathrm{d}s. \end{aligned} \tag{3.11}$$

Let us define

$$\left\{u, \int_0^T b_{12}(T-s)u(s)\,\mathrm{d}s = \tau_1\tau_2 D, u(t) = D, t \in [T, T+R]\right\} = \mathcal{U}_D.$$

For a small τ, consider $u + \tau\phi \in \mathcal{U}_D$, i.e.

$$\phi \in \left\{\phi, \int_0^T \exp(s/\tau_1)\phi(s)\,\mathrm{d}s = 0, \right.$$
$$\left. \int_0^T \exp(s/\tau_2)\phi(s)\,\mathrm{d}s = 0, \phi(t) = 0, \text{ for } t \in [T, T+R]\right\} = \mathcal{U}_D^0.$$

The first two constraints in $\mathcal{U}_D^0$ are from equation (3.10). We then have

$$\frac{\mathrm{d}I(u+\tau\phi)}{\mathrm{d}\tau}\Big|_{\tau=0} = 0$$

which gives

$$\int_0^T \left\{\left[\int_0^{T+R} b_{12}^2(t-s)\,\mathrm{d}t\right] |u(s)|^{2\alpha-1} \operatorname{sgn}(u(s))\phi(s)\right\} \mathrm{d}s = 0. \tag{3.12}$$

Comparing equation (3.12) with the first two constraints in $\mathcal{U}_D^0$, we conclude that

$$\left[\int_0^{T+R} b_{12}^2(t-s)\,\mathrm{d}t\right] |u(s)|^{2\alpha-1} \operatorname{sgn}(u(s)) = \lambda \exp\left(\frac{s}{\tau_1}\right) + \mu \exp\left(\frac{s}{\tau_2}\right) \tag{3.13}$$

for $s \in [0, T]$ with two parameters $\lambda, \mu \in R$. Hence the solution of the original problem is

$$u(s) = \frac{\left|\lambda \exp\left(\frac{s}{\tau_1}\right) + \mu \exp\left(\frac{s}{\tau_2}\right)\right|^{1/(2\alpha-1)} \operatorname{sgn}\left[\lambda \exp\left(\frac{s}{\tau_1}\right) + \mu \exp\left(\frac{s}{\tau_2}\right)\right]}{\left(\int_0^{T+R} b_{12}^2(t-s)\,\mathrm{d}t\right)^{1/(2\alpha-1)}} \tag{3.14}$$

with λ, μ being given by

$$\begin{cases} D\tau_2 \exp\left(\frac{T}{\tau_2}\right) = \int_0^T \exp\left(\frac{s}{\tau_2}\right) \\ \quad \times \dfrac{\left|\lambda \exp\left(\frac{s}{\tau_1}\right) + \mu \exp\left(\frac{s}{\tau_2}\right)\right|^{1/(2\alpha-1)} \operatorname{sgn}\left[\lambda \exp\left(\frac{s}{\tau_1}\right) + \mu \exp\left(\frac{s}{\tau_2}\right)\right]}{\left(\int_0^{T+R} b_{12}^2(t-s)\,\mathrm{d}t\right)^{1/(2\alpha-1)}} \mathrm{d}s \\ D\tau_1 \exp\left(\frac{T}{\tau_1}\right) = \int_0^T \exp\left(\frac{s}{\tau_1}\right) \\ \quad \times \dfrac{\left|\lambda \exp\left(\frac{s}{\tau_1}\right) + \mu \exp\left(\frac{s}{\tau_2}\right)\right|^{1/(2\alpha-1)} \operatorname{sgn}\left[\lambda \exp\left(\frac{s}{\tau_1}\right) + \mu \exp\left(\frac{s}{\tau_2}\right)\right]}{\left(\int_0^{T+R} b_{12}^2(t-s)\,\mathrm{d}t\right)^{1/(2\alpha-1)}} \mathrm{d}s. \end{cases} \tag{3.15}$$

We arrive at the following conclusions.

Theorem 1. *For the hold-on control problem with $\alpha > 1/2$, its unique optimal control signal is given by equation (3.14) with mean trajectory and mean velocity given by equation (3.5).*

Proof. We only need to prove the uniqueness of the solution of equation (3.15), which is quite straightforward and we leave it to the reader. □

Now we take into account various cases of the model. We first assume $\alpha = 1$, the case considered in [9] and other publications [27].

3.1. Case of $\alpha = 1$

Let us define

$$\begin{aligned} H(s) &= \int_0^{T+R} b_{12}^2(t-s)\,\mathrm{d}t \\ &= \frac{\tau_1^2\tau_2^2}{(\tau_2-\tau_1)^2}\left\{-\frac{\tau_2}{2}\left[\exp\left(-\frac{2}{\tau_2}(T+R-s)\right)-\exp\left(\frac{2}{\tau_2}s\right)\right]\right. \\ &\quad +\frac{2\tau_1\tau_2}{\tau_1+\tau_2}\left[\exp\left(-\frac{\tau_1+\tau_2}{\tau_1\tau_2}(T+R-s)\right)-\exp\left(\frac{\tau_1+\tau_2}{\tau_1\tau_2}s\right)\right] \\ &\quad \left.-\frac{\tau_1}{2}\left[\exp\left(-\frac{2}{\tau_1}(T+R-s)\right)-\exp\left(\frac{2}{\tau_1}s\right)\right]\right\}. \end{aligned}$$

(λ, μ) is now the solution of the following equation:

$$\begin{cases} \lambda\int_0^T \dfrac{\exp\left(\frac{s}{\tau_2}+\frac{s}{\tau_1}\right)}{H(s)}\,\mathrm{d}s + \mu\int_0^T \dfrac{\exp\left(\frac{2s}{\tau_2}\right)}{H(s)}\,\mathrm{d}s = \tau_2 D\,\exp\left(\frac{T}{\tau_2}\right) \\ \lambda\int_0^T \dfrac{\exp\left(\frac{2s}{\tau_1}\right)}{H(s)}\,\mathrm{d}s + \mu\int_0^T \dfrac{\exp\left(\frac{s}{\tau_1}+\frac{s}{\tau_2}\right)}{H(s)}\,\mathrm{d}s = \tau_1 D\,\exp\left(\frac{T}{\tau_1}\right). \end{cases} \tag{3.16}$$

Therefore (λ, μ) is given by

$$\begin{pmatrix}\lambda\\ \mu\end{pmatrix} = \Sigma^{-1}\begin{pmatrix}\tau_2 D\,\exp(T/\tau_2)\\ \tau_1 D\,\exp(T/\tau_1)\end{pmatrix} \tag{3.17}$$

where

$$\Sigma = \begin{pmatrix} \int_0^T \dfrac{\exp\left(\frac{s}{\tau_2}+\frac{s}{\tau_1}\right)}{H(s)}\,\mathrm{d}s & \int_0^T \dfrac{\exp\left(\frac{2s}{\tau_2}\right)}{H(s)}\,\mathrm{d}s \\ \int_0^T \dfrac{\exp\left(\frac{2s}{\tau_1}\right)}{H(s)}\,\mathrm{d}s & \int_0^T \dfrac{\exp\left(\frac{s}{\tau_1}+\frac{s}{\tau_2}\right)}{H(s)}\,\mathrm{d}s \end{pmatrix}.$$

Therefore

$$u(s) = \begin{cases} [\lambda\exp(s/\tau_1)+\mu\exp(s/\tau_2)]/H(s) & \text{if} \quad s\in[0,T] \\ D & \text{otherwise.} \end{cases} \tag{3.18}$$

Now we are in the position to discuss many interesting issues about the optimal control signal, its velocity, trajectory etc.

The first issue we intend to address is the impact of the length of R on the model behaviour. From [9], it seems that they claimed the final outcome of the model depends on R and a quite large R is required. In figure 1, we plot control signals and mean velocity versus time. It is easily seen that the control signal depends on R: the longer the R is, the more monotonic the

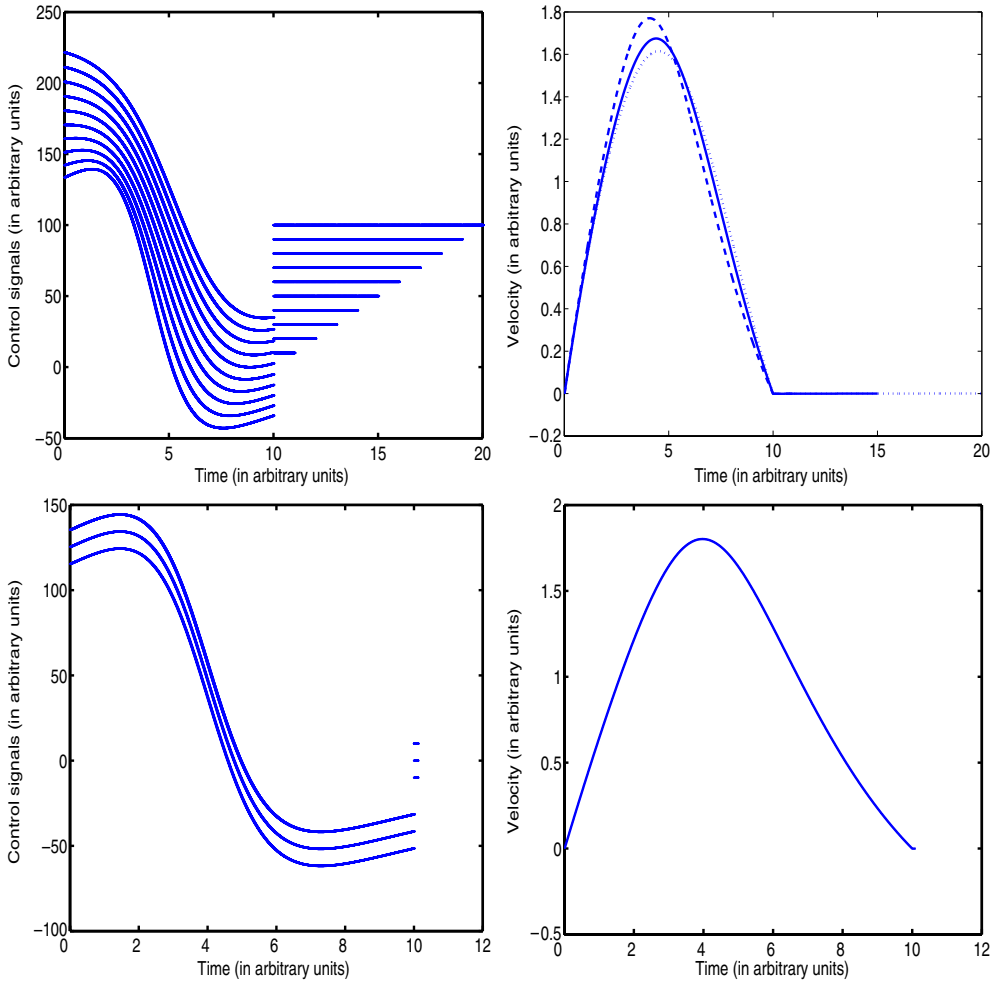

Figure 1. Control signals and mean velocity with $r = 1, 2, \ldots, 10$ (upper panel), and $R = 0.1$, $0.05, 0.01$ (bottom panel). Control signals move upwards with 10 units when $R = 2, 3, \ldots, 10$ and downwards with 10 units with $R = 0.05, 0.01$. For mean velocity only $r = 1$ (dashed line), 5 (solid line) and 10 (dotted line) are shown.

control signal. Nevertheless, the dependence of the velocity on R is not substantial and so is the trajectory (not shown). In particular, when R tends to zero, we see that

$$u_0(t) = \lim_{R \to 0} u(t)$$

exists (we leave the proof of it to the reader), as numerically shown in figure 1. When $R = 0.1, 0.05, 0.01$, the control signals and velocity for different R are almost identical and the velocity takes the bell shape.

Another interesting issue is to define

$$u(t) = u_1(t) + u_2(t)$$

with $u_1(t) > 0$ and $u_2(t) < 0$, corresponding to the solution equation (3.14) defined in theorem 1. In figure 2 we plot the control signals $u(t), u_1(t)$ and $u_2(t)$. It is interesting to note that the maximum of $u_2(t)$ is attained before $u_1(t)$ reaches its minimum. Again this

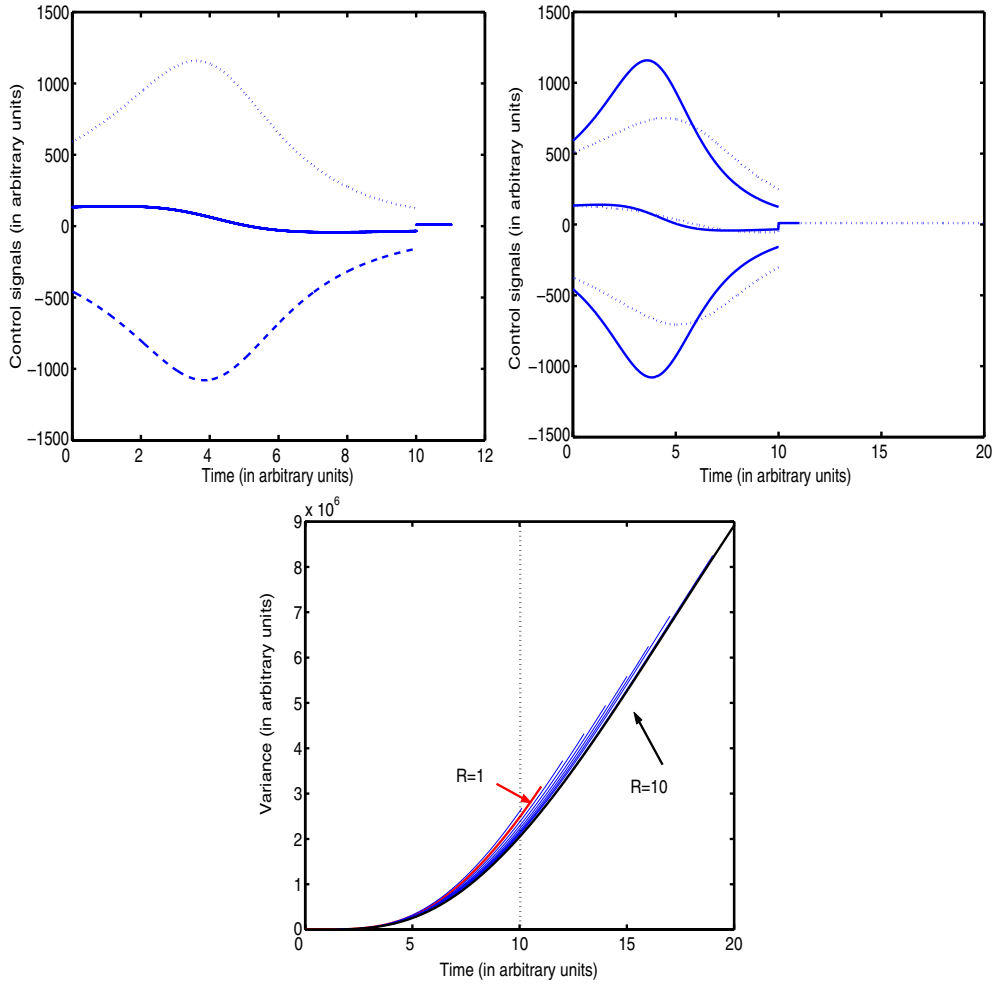

Figure 2. Control signal and variance versus time. *Upper panel (left)*: $u(t)$ (solid line), $u_2(t)$ (dashed line) and $u_1(t)$ (dotted line) versus time with $T = 10$, $R = 1$. It is found $(\lambda, \mu) = (e^4(-6.2918, 8.1321))$. *Upper panel (right)*: u_1, u_2, u with $R = 1$ (solid lines, see left), with $R = 10$ (dotted lines). *Bottom panel*: variances with $R = 0.1, 1, 2, \ldots, 10$.

agrees with the general principle in neuroscience: excitatory signals are the driving signals and inhibitory signals are the followers. Furthermore the inhibitory signals show the 'push–pull' phenomenon: the bigger the excitatory signals are, the bigger the inhibitory signals (absolute value). We have seen that the mean trajectory, velocity and control signals are not sensitive to the hold-on period R, but u_1 and u_2 are quite sensitive to R, as shown in figure 2.

One of our future tasks is to implement neuronal control signals $u_1(t)$ and $u_2(t)$ via a spiking neuronal network. We call them sub-control signals. Note that the decomposition of $u(t)$ into $u_1(t)$ and $u_2(t)$ is completely different from the results reported in [9]. In [9], they define $\bar{u}_1(t) = u(t)I_{\{u(t)>0\}}$ and $\bar{u}_2(t) = u(t)I_{\{u(t)<0\}}$, in terms of a purely phenomenological observation. Our decomposition here might reveal more fundamental principles behind the optimal control problem. According to our definition of sub-control signals, we have $u_2(t) = \lambda \exp(s/\tau_1)/H(s) < 0$ and $u_1(t) = \mu \exp(s/\tau_2)/H(s) > 0$ (see figure 2). It is not

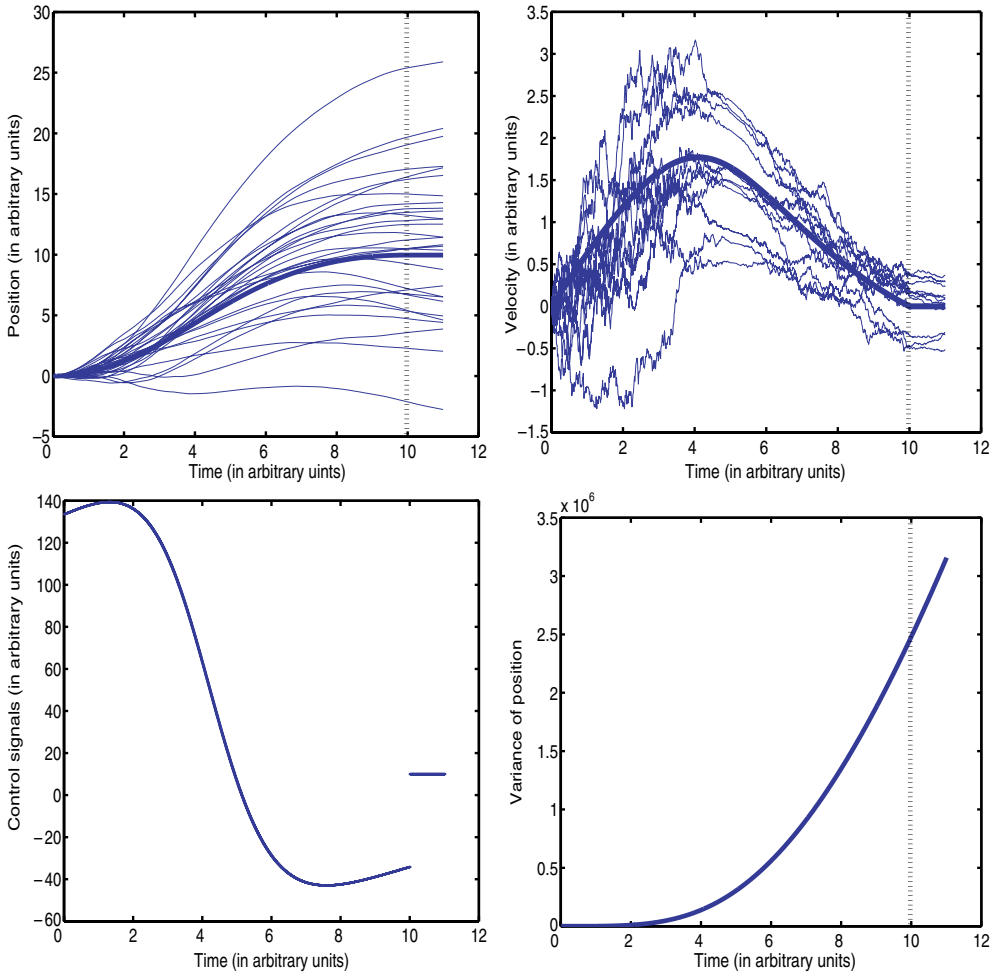

Figure 3. Position, velocity, control signal and variance versus time. *Upper panel left (position)*: thick line is the average position ($\langle x_1(t)\rangle$) and thin lines are realizations ($x_1(t)$). *Upper panel right (velocity)*: thick line is the average velocity ($\langle x_2(t)\rangle$) and thin lines are realizations ($x_2(t)$). *Bottom panel*: left is the control signal and right is variance of position. Parameters are $T = 10$, $R = 1$, $D = 10$, $\tau_1 = 10$ and $\tau_2 = 100$.

surprising to see that with increasing R, the sub-control signal is reduced, and correspondingly, the variance of trajectory is reduced (figure 2).

3.2. *Cases of* $\alpha \neq 1, \alpha > 1/2$

It is interesting to compare the results of various α. As we have mentioned before, when $\alpha = 1/2$ it corresponds to the Poisson input case. Roughly speaking, the larger the α is, the more randomness the neuron fires.

In agreement with results in figure 1 in [6], we see that the variance is a decreasing function of α. The larger the α is, the smaller the variance of the trajectory. Comparing the figure of bottom panel right in figure 3 with figure 4, we see that the variance is dramatically

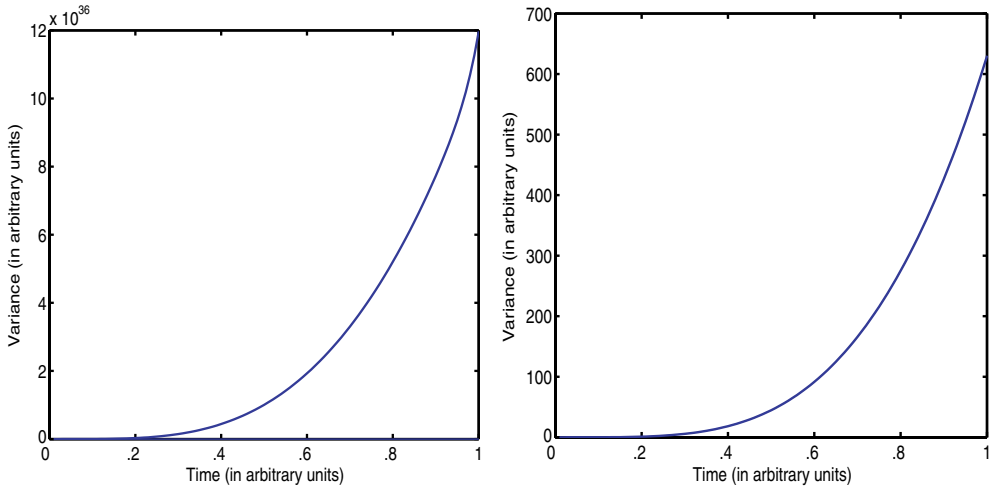

Figure 4. Variance of trajectory with $\alpha = 0.6$ (left) and $\alpha = 1.4$ (right).

reduced with a slight increasing of α (from 0.6 to 1.4). Remember that the larger the α is, the more randomness the neuron fires. Our simulation results tell us that to obtain an accurate end point of movement, the neuron should operate very randomly (with large α). Of course, we should remind ourselves that the control signals $u(s)$ correspond to the firing rate of neurons. To obtain a reasonable estimate of the firing, we have to keep α small. Hence the nervous system should find a trade-off between reducing the movement variance (increasing α) and accurately estimating the firing rates (decreasing α).

3.3. $0 < \alpha \leqslant 1/2$

From equation (3.11) we see that when $\alpha < 1/2$, and if $u(s) = \delta_y(s)$, the delta function at y, we will have

$$I(u) = 0$$

which is of course the minimum point of the variance. To satisfy the constraints, we could define

$$u^*(s) = a_1\delta_{y_1}(s) + a_2\delta_{y_2}(s) \qquad y_1 \neq y_2,\ y_1, y_2 \in [0, T]$$

with appropriate constants a_1 and a_2 so that the constraint is fulfilled and we will have

$$I(u^*) = 0$$

as well. Hence when $\alpha < 1/2$, the optimal control signal is not unique.

When $\alpha = 1/2$, from equation (3.11), we see that if we define

$$u(s) = \delta_{y_0}(s)$$

then $I(u)$ will attain its global minimum, where y_0 is the minimum point of $H(s)$ (see figure 5). Therefore we can define

$$u(s) = a_1\delta_{y_0}(s) + a_2\delta_{y_0+\epsilon}(s)$$

for a parameter ϵ, and $I(u)$ will approach its global minimum when ϵ tends to zero.

In conclusion, when $\alpha \leqslant 1/2$, the control signal is degenerate.

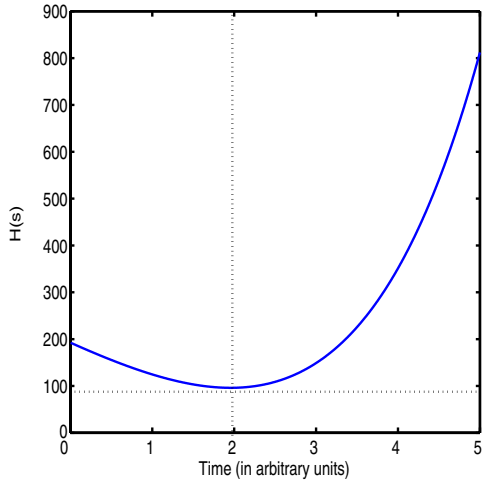

Figure 5. The function H versus time. The cross point of the vertical-dotted and horizontal-dotted lines is the minimum point of $H(s)$.

3.4. Instantaneous constraint

As we have mentioned in the previous section, the original control problem is a hold-on control, i.e. we hold on the moving trajectory at the end of its movement. What form of the solution will be if we release the hold-on constraint? In other words, we consider the following control problem.

Control with an instantaneous constraint. Find $u(s) \in \mathcal{L}^{2\alpha}[0, T + R]$ which minimizes

$$\int_T^{T+R} \left[\int_0^t b_{12}^2(t-s)u(s)^{2\alpha}\,\mathrm{d}s \right] \mathrm{d}t \tag{3.19}$$

subject to the constraint

$$\begin{cases} \langle x_1(T)\rangle = \int_0^T b_{12}(T-s)u(s)\,\mathrm{d}s = \tau_1\tau_2 D & \text{and} \\ \langle x_2(T)\rangle = \int_0^T b_{22}(T-s)u(s)\,\mathrm{d}s = 0. \end{cases} \tag{3.20}$$

Theorem 2. *For the hold-on control problem with the instantaneous constraints, its unique optimal control signal is given by equation (3.14) with mean trajectory and mean velocity given by equation (3.5).*

Proof. By noting that the constraints in equation (3.20) is equivalent to equations (3.6) and (3.7) with $t = T$, which implies equation (3.10), the conclusions of the theorem follow. □

Basically theorem 2 tells us that the hold-on constraint is equivalent to the instantaneous constraint of equation (3.20). From theorems 1 and 2, one might conclude that the bell shape velocity automatically follows from the requirement of the vanishing velocity at time T. To see whether this is true, we turn our attention to another form of optimization, but with identical constraints in the next section.

4. End-point minimization of variance

In the control problem, discussed in the previous section, we see that the variance between $[T, T + R]$ is minimized. Suppose that our primary purpose of control is to have a trajectory which exhibits small variance, in particular at the end point T. The requirement leads to the following control problem.

End-point control. Find $u(s) \in \mathcal{L}^{2\alpha}[0, T]$ which minimizes

$$\int_0^T \left[b_{12}^2(T-s)u(s)^{2\alpha}\right] \mathrm{d}s \tag{4.1}$$

subject to the constraint

$$\int_0^t b_{12}(t-s)u(s)\,\mathrm{d}s = \tau_1\tau_2 D \qquad \text{for} \quad t \in [T, T+R]. \tag{4.2}$$

It is straightforward to see that we have the following conclusions.

Theorem 3. *The optimal control signal with the end-point control is given by*

$$u(s) = \frac{\left|\lambda \exp\left(\frac{s}{\tau_1}\right) + \mu \exp\left(\frac{s}{\tau_2}\right)\right|^{1/(2\alpha-1)} \operatorname{sgn}\left[\lambda \exp\left(\frac{s}{\tau_1}\right) + \mu \exp\left(\frac{s}{\tau_2}\right)\right]}{\left(b_{12}^2(T-s)\right)^{1/(2\alpha-1)}} \tag{4.3}$$

with λ, μ *satisfying*

$$\begin{cases} D\tau_2 \exp\left(\frac{T}{\tau_2}\right) = \int_0^T \exp\left(\frac{s}{\tau_2}\right) \\ \quad \times \dfrac{\left|\lambda \exp\left(\frac{s}{\tau_1}\right) + \mu \exp\left(\frac{s}{\tau_2}\right)\right|^{1/(2\alpha-1)} \operatorname{sgn}\left[\lambda \exp\left(\frac{s}{\tau_1}\right) + \mu \exp\left(\frac{s}{\tau_2}\right)\right]}{\left(b_{12}^2(T-s)\right)^{1/(2\alpha-1)}}\,\mathrm{d}s \\ D\tau_1 \exp\left(\frac{T}{\tau_1}\right) = \int_0^T \exp\left(\frac{s}{\tau_1}\right) \\ \quad \times \dfrac{\left|\lambda \exp\left(\frac{s}{\tau_1}\right) + \mu \exp\left(\frac{s}{\tau_2}\right)\right|^{1/(2\alpha-1)} \operatorname{sgn}\left[\lambda \exp\left(\frac{s}{\tau_1}\right) + \mu \exp\left(\frac{s}{\tau_2}\right)\right]}{\left(b_{12}^2(T-s)\right)^{1/(2\alpha-1)}}\,\mathrm{d}s \end{cases} \tag{4.4}$$

where $\alpha > 1/2$.

Proof. The proofs are quite similar to the proof of theorem 1 and we omit them here. □

Figure 6 tells us that the variance is dramatically reduced at the end point, with the end-point control, in comparison with the hold-on control. However, from figure 6 we could conclude that for the end-point control, its velocity profile is not symmetric. It increases to its maximum value when the time approaches T and suddenly drops to zero when $t = T$.

Whether the bell shape of the velocity in the hold-on control is a generic property of the control or it depends on various model parameters? To theoretically prove such a conclusion, we need to show that there is only a unique maximum point for the velocity. In fact, figure 7 clearly shows that the conclusion is not true. In figure 7, we see that the velocity has two extreme points: one minimum and one maximum, provided that T is large. In figure 7 (right), the critical value of T at which the velocity exhibits two extreme values is depicted, i.e. a bifurcation diagram. We see that the critical value of T is between $T = 16$ and $T = 17$. In other words, the bell shape velocity is observable with a relatively small T. One could of course argue that physiologically reasonable parameter regions are the regions on the left-hand side of the vertical dashed line in figure 7 (right), i.e. $T < 16$. Comparing the velocity of the hold-on control with the end-point control, we see that for the hold-on control the velocity is

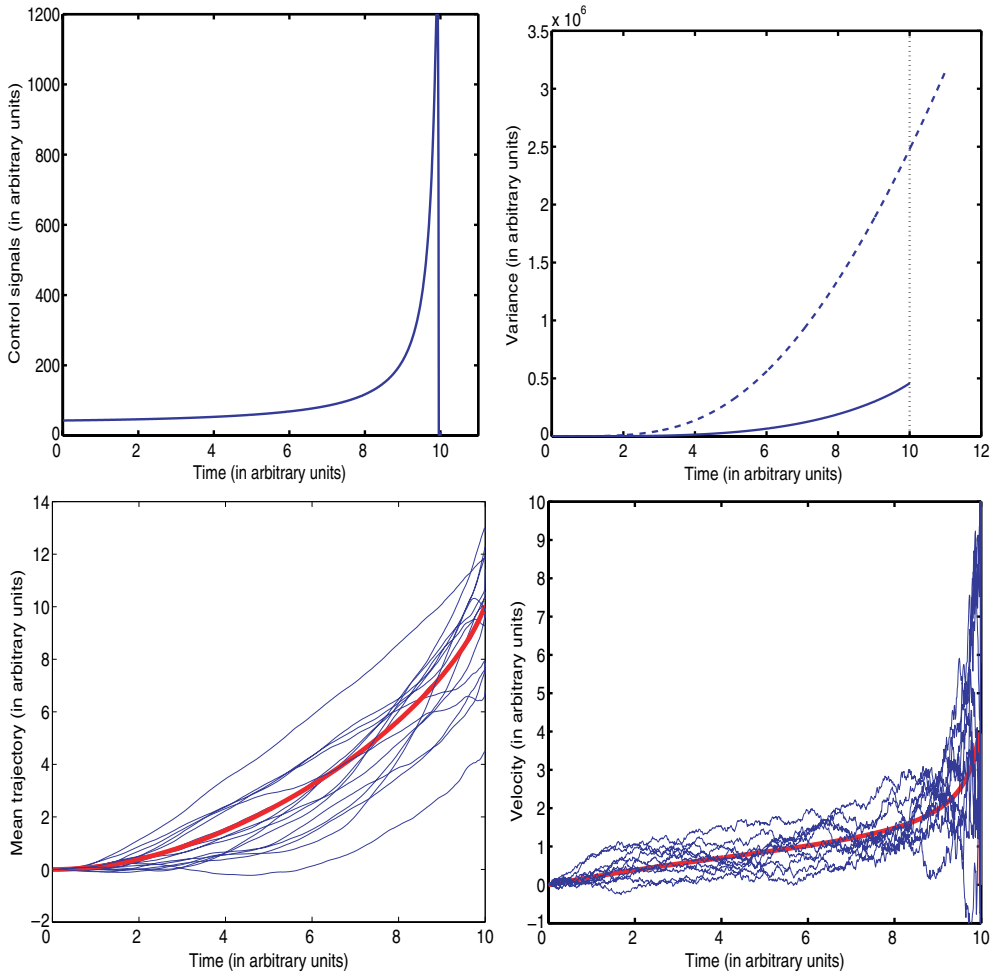

Figure 6. Control signals of the end-point minimization, variance, mean trajectory (thick line), realizations of trajectory, mean velocity (thick line) and realizations of velocity versus time.

first negative and then positive; but for the end-point control the velocity is first positive and then negative. In other words, in the end-point control, the trajectory shows the phenomenon of overshooting: the trajectory surpasses the desired point and then returns to the desired point.

5. Discussion

We have presented a rigorous study on the TOPS model. Although TOPS models have been attracting considerable attention, to the best of our knowledge, an analytical treatment as we developed here has not been reported in the literature. As we clearly demonstrated here, such a theoretical study can shed many new lights on the model and its implications.

We have only considered open-loop control in the current paper. It is interesting to consider the similar problem with a feed back control, as we mentioned in [6]. To completely solve the control problem with a feed back is a formidable task, as it has been demonstrated

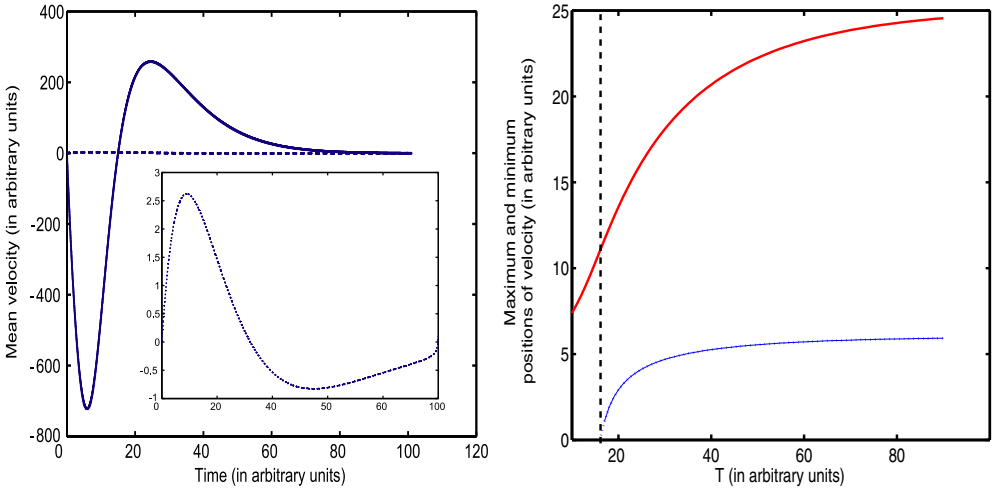

Figure 7. Mean velocity of the hold-on and the end-point minimization versus time and bifurcation diagram of the maximum and minimum points of mean velocity of the hold-on control. *Left*: solid line is the hold-on control, dotted line is end-point control. Inset is the blow up of the control signal of the end-point control. $T = 100$, $R = 1$. *Right*: bifurcation diagram of the maximum and minimum points of the mean velocity of the hold-on control with $T = [10, 100]$. Upper branch is the position of maximum point and bottom branch is the minimum point.

in mathematical financial problems [14, 19]. In our further work, we intend to tackle the issue with a linear feedback. The movement model becomes a geometrical Brownian motion. It has been extensively studied in the context of the Black–Shore model.

Another interesting issue is to implement the control task by, say at least, (spiking) integrate-and-fire neuronal networks [3, 4]. It is then interesting to implement it both as a rate coding and a time coding model. For time coding model, our results here can be directly applicable ($\alpha > 1/2$). For rate coding model, it is still problematic since we will face a situation with $\alpha < 1/2$.

As we have pointed out before, whether $\alpha = 1$ or not is a debatable issue and is related to the currently hotly discussed problem of rate coding and time coding (see, for example, [8, 16]). With $\alpha = 1$, the output signal is not the firing rate generated from a Poisson process. More exactly, with a Poisson process, we should have $\alpha = 1/2$. Of course, if we assume that the information of motor movement is carried by the interspike intervals of a spike train, then we should have $\alpha = 1$ for the Poisson process. On the surface, our work is purely an optimal control problem. Our actual motivation is to combine neuronal outputs with motor tasks, and we expect such an approach would eventually help us to understand the puzzling issue of neuronal coding. To completely and finally resolve the issue, we have to resort to experimental results.

In summary, our approach answers some questions related to the TOPS models and also opens up many illuminating issues to be further investigated.

Finally we intend to compare the results in the current paper with that obtained in [6]. In [6], the optimal control problem for the following model:

$$\mathrm{d}X_t = -\partial H(X_t, t)/\partial X_t + \eta_2(t)\,\mathrm{d}B_t \tag{5.1}$$

is considered with a specific form (potential) H as defined in [6]. However, as we all know from classical physics, equation (2.1) is a more realistic physical model than equation (5.1) because, recalling Newton's laws of motion, a potential really acts to cause a change in velocity

rather than in position. The optimal control problem defined by equation (5.1) has been widely studied in the literature [19] due to its simplicity, i.e. it is not a degenerate diffusion process. Equation (2.1) is totally different, it is a degenerate diffusion process: the diffusion coefficient in the equation of x_1 is zero. This makes the task, i.e. to analytically find out an optimal control signal, much hard. In fact, the well-known theory of the stochastic optimal control cannot be applied to the optimal control problem defined by equation (2.1) [19]. Of course, using the speeded-up approximation, we can approximate equation (2.1) by equation (5.1) (see p 178 in [1] for more details).

Acknowledgments

JF was partially supported by grants from UK EPSRC(GR/R54569), (GR/S30443) and (GR/S20574) and a grant of the Royal Society.

References

[1] Aldous D 1989 *Probability Approximations via the Poisson Clumping Heuristic* (New York: Springer)
[2] van Beers R J, Baraduc P and Wolpert D M 2002 Role of uncertainty in sensorimotor control *Philos. Trans. R. Soc.* B **357** 1137–45
[3] Feng J F 2001 Is the integrate-and-fire model good enough?—*a* review *Neural Netw.* **14** 955–75
[4] Feng J F 2002 *Computational Neuroscien—A Comprehensive Approach* ed J Feng (Boca Raton, FL: CRC)
[5] Feng J F, Tartaglia G G and Tirozzi B 2001 A note on minimum-variance theory and beyond submitted
[6] Feng J F, Zhang K W and Wei G 2002 Towards a mathematical foundation of minimum-variance theory *J. Phys. A: Math. Gen.* **35** 7287–304
[7] Flash T and Sejnowski T J 2001 Computational approaches to motor control *Curr. Opin. Neurobiol.* **11** 655–62
[8] Harris K D, Henze D A, Hirase H, Leinekugel X, Dragoi G, Czurko A and Buzsaki G 2002 Spike train dynamics predicts theta-related phase precession in hippocampal pyramidal cells *Nature* **417** 738–41
[9] Harris C M and Wolpert D M 1998 Signal-dependent noise determines motor planning *Nature* **394** 780–4
[10] Kitazawa S 2002 Optimization of goal-directed movements in the cerebellum: a random walk hypothesis *Neurosci. Res.* **43** 289–94
[11] Jones K E, Hamilton A F D and Wolpert D M 2002 Sources of signal-dependent noise during isometric force production *J. Neurophysiol.* **88** 1533–44
[12] Ivanenko Y P *et al* 2002 Two-thirds power law in human locomotion: role of ground contact forces *Neuroreport* **13** 1171–4
[13] Kawato M 1999 Internal models for motor control and trajectory planning *Curr. Opin. Neurobiol.* **9** 718–27
[14] Kushner H J 1999 Consistency issues for numerical methods for variance control, with applications to optimization in finance *IEEE Trans. Autom. Control* **44** 2283–96
[15] Lynch K M *et al* 2002 Motion guides for assisted manipulation *Int. J. Robot. Res.* **21** 27–43
[16] Mehta M R, Lee A K and Wilson M A 2002 Role of experience and oscillations in transforming a rate code into a temporal code *Nature* **417** 741–6
[17] Mazurek M E and Shadlen M N 2002 Limits to the temporal fidelity of cortical spike rate signals *Nat. Neurosci.* **5** 463–71
[18] Novak K E, Miller L E and Houk J C 2002 The use of overlapping submovements in the control of rapid hand movements *Exp. Brain Res.* **144** 351–64
[19] Oksendal B 1989 *Stochastic Differential Equations* 2nd edn (Berlin: Springer)
[20] Ricciardi L M and Sato S 1990 Diffusion process and first-passage-times problems *Lectures in Applied Mathematics and Informatics* ed L M Ricciardi (Manchester: Manchester University Press)
[21] Richardson M J E and Flash T 2002 Comparing smooth arm movements with the two-thirds power law and the related segmented-control hypothesis *J. Neurosci.* **22** 8201–11
[22] Sejnowski T J 1998 Making smooth moves *Nature* **394** 725–6
[23] Shadlen M N and Newsome W T 1994 Noise, neural codes and cortical organization *Curr. Opin. Neurobiol.* **4** 569–79
[24] Shin J 2002 The noise shaping neural coding hypothesis: a brief history and physiological implications *Neurocomputing* **44** 167–75

[25] Smeets J B J, Frens M A and Brenner E 2002 Throwing darts: timing is not the limiting factor *Exp. Brain Res.* **144** 268–74
[26] Takikawa Y *et al* 2002 Modulation of saccadic eye movements by predicted reward outcome *Exp. Brain Res.* **142** 284–91
[27] Todorov E 2002 Cosine tuning minimizes motor errors *Neural Comput.* **14** 1233–60
[28] Tuckwell H C 1988 *Introduction to Theoretical Neurobiology* vol 2 (Cambridge: Cambridge University Press)
[29] Wolpert D M and Ghahramani Z 2000 Computational principles of movement neuroscience *Nat. Neurosci.* **3** 1212–7